




Calculation of the shape of energy-ordered spectra for investigations of the nuclear continuum

J. R. Pinzón ^{1,*}, W. Rodríguez ^{2,1} and F. Cristancho ¹

¹Universidad Nacional de Colombia, Sede Bogotá, Facultad de Ciencias, Departamento de Física, Bogotá, Colombia

²Pontificia Universidad Javeriana, Facultad de Ciencias, Departamento de Física, Bogotá, Colombia



(Received 1 March 2020; accepted 4 November 2020; published 28 December 2020)

The nuclear continuum may potentially be investigated by means of fusion-evaporation reactions in combination with the Hk technique. The γ radiation in such experiments can be analyzed using energy ordering which produces complex spectra. A method for computing the shape of the energy-ordered spectra is presented and benchmarked by reproducing simulated data. The spectrum shape computation is applied to experimentally relevant cases and is used for extracting the level density parameter from simulations. Furthermore, the calculation shows to be useful for the characterization of nuclear phase transitions.

DOI: [10.1103/PhysRevC.102.064325](https://doi.org/10.1103/PhysRevC.102.064325)

I. INTRODUCTION AND MOTIVATION

There is a large variety of phenomena that can be studied from nuclei in the continuum region, typically above the particle threshold where the quantum levels overlap due to their proximity. For instance, thermodynamic quantities used to describe the nucleus in the continuum, can be related with structural quantities such as deformation parameters [1–5], which makes this region a very attractive field of study offering rich and new physics to explore. Nevertheless during the last decades most of the experimental studies of nuclei have been intended to understand the behavior in the discrete region, or in the quasicontinuum where the experimental resolution does not allow one to differentiate between nonoverlapping levels. Thus the investigation of the nuclear continuum remains one of the most challenging fields from both theoretical and experimental sides.

Different experimental techniques have been used to study the continuum and quasicontinuum region, for example to measure γ strength functions [6]. One of this techniques is the Oslo method [7], which uses transfer or inelastic scattering reactions together with particle- γ coincidence for obtaining the spectra of radiation coming from the quasicontinuum region. This methodology has been used to obtain level densities and γ strength functions of several nuclei [8–15]. A recently developed theoretical formalism [16] to simultaneously determine level densities and γ strengths has met good agreement with the experimental data extracted by the Oslo group for $^{170-172}\text{Yb}$ [11]. This result invalidates the time-honored Brink-Axel hypothesis for γ strengths, showing that this kind of investigation has truly the chance of touching on new physics. Nevertheless, the mandatory use of transfer reactions limits the nuclei that can be studied by using this methodology since only low spin states can be populated with such reactions. Therefore, theoretical predictions of nuclear phase transitions as the one in Ref. [17], as well as of higher spin states

computed with the formalism in Ref. [16], cannot be experimentally tested yet. More experimental techniques are still required to overcome the limitations of the already existing methods, as well as to complement the available databases [6].

A method which may potentially overcome this limitation is based on fusion-evaporation reactions that populate high spin and energy states in the continuum region. It was shown by numerical simulations from the γ decay that *energy-ordered spectra* (EOS) can be used to study the nuclear properties of the continuum states [18]. Additionally the Hk technique could be used to extract EOS from different (spin, energy) regions in the continuum [19,20]. Therefore the combination of both techniques, Hk -EOS, constitutes a promising tool in the development of a new experimental technique for the continuum region. In this work, a calculation of the EOS shape is presented and applied to the extraction of physical parameters describing the continuum region.

Nuclear properties can be inferred from the γ emission following Fermi's golden rule,

$$\text{emission probability} \propto f(E_\gamma) E_\gamma^3 \frac{\rho_f}{\rho_i}, \quad (1)$$

where $f(E_\gamma)$ is the *gamma strength*, E_γ is the energy of the γ ray, and $\rho_{f/i}$ is the final/initial *level density*. For the transitions under consideration, the electric dipole $E1$ provides the largest contribution to EOS [18] and is well described by the giant dipole resonance [21], for which we will assume validity of the Brink-Axel hypothesis [22,23], according to the formulation in Ref. [24]. The level density is described with the Fermi gas model including the *level density parameter* a [25]. This is a relevant physical quantity for describing the nucleus, and one of the main focuses of this work.

Relating the γ radiation to Eq. (1) requires isolating the radiation originated from a certain nuclear excitation energy E and spin I . Experimentally, this implies two challenges: (i) the identification of the entry state and (ii) the selection of the primary radiation or first γ ray of each cascade.

The first task can be achieved using the Hk technique which allows to perform gates in (I, E) regions [20]. By

*jrpinzona@unal.edu.co

considering the response function of an experimental array, measured (k, H) points are converted to an (I, E) distribution as it was demonstrated for the GASP array [19].

The second task cannot be accomplished because of limitations in the presently available electronics, which is unable to distinguish the temporal order of emitted γ rays due to the short time span in which a cascade is emitted. If this restriction was not present, one could order the γ rays in a cascade by their emission time and then produce *time-ordered* spectra by histogramming the first emitted ones. The first-emitted spectrum would correspond to the primary radiation. This is, however, not feasible. One can instead order the γ rays in a cascade by their energies [20] and then produce an *energy-ordered spectrum* (EOS) by classifying the most energetic ones in one spectrum. This is then taken as a working approximation to the primary radiation [18].

Previous works showed that it is possible to extract from EOS physical parameters describing the nucleus. In Ref. [18], the level density parameter was extracted from a fit to the high energy tail of EOS. Although this method provided values in agreement with the input to simulations, the uncertainties were large since only a reduced part of the spectra was used and information at low transition energies was disregarded. In Refs. [26,27], more advanced mathematical tools such as order statistics [28] and extreme value theory [29] were applied for the calculation of the spectra in the entire energy range. Although the fit was not optimal, these works contributed to a better understanding of EOS formation.

A major step towards the modeling of EOS was performed in Ref. [30]. A detailed probability calculation provided a mathematical function working in the entire energy range. Nevertheless, such a function was computed and tested in the *spin-independent case*, meaning that no spin dependence of the transition probabilities was considered. In the present work, the calculated *spectrum shape* is reviewed and extended to include spin dependency (*spin-dependent case*). This approach is validated by a comparison with spectra produced by a simulation of the nuclear continuum decay carried out with the code GAMBLE [31], which includes all the known variables deciding on the evolution of the decay process. Wide distributions of entry states can also be given as input, allowing to account for the experimental conditions given by the *Hk* technique.

In Sec. II the spin-independent calculation of the spectrum shape is reviewed. In Sec. III the extension to the spin-dependent case is discussed and the result of the calculation is compared with a simulated spectrum. In Sec. IV distributions of initial states are included. In Sec. V, the level density parameter is extracted from fits to EOS and the quality of the calculation is assessed. In Sec. VI an example of a nuclear phase transition is analyzed using the spectrum shape calculations. The summary and conclusions are presented in Sec. VII.

II. SPECTRUM SHAPE FOR THE SPIN-INDEPENDENT CASE

In the spin-independent case, the probability density of γ emission p depends only on the *intrinsic excitation energy* U

and the γ energy E_γ . Following Eq. (1), p can be written

$$p(E_\gamma, U) = \frac{\phi(E_\gamma, U)}{F(U)} \quad (2)$$

with ϕ as the non-normalized probability density function,

$$\phi(E_\gamma, U) = f(E_\gamma)E_\gamma^3 \rho(U - E_\gamma), \quad (3)$$

and F its cumulative function

$$F(U) = \int_0^U dE_\gamma \phi(E_\gamma, U). \quad (4)$$

For initial states with an intrinsic excitation energy U , Eq. (2) gives the E_γ distribution of the first emitted γ rays, corresponding to the time-ordered spectrum.

Precisely, the difficulty in predicting EOS lies in the fact that the most energetic γ ray is not necessarily emitted first, and hence its distribution is not given by Eq. (2) as such transitions do not necessarily occur at the initial U . In Ref. [30], the energy distribution of the most energetic γ rays or spectrum shape, p_{EOS} , was computed for the spin-independent case. For an initial intrinsic excitation energy U , the spectrum shape is obtained by considering only the first n γ rays of each cascade. This is expressed by the summation

$$p_{\text{EOS}}(E_\gamma, U) = \sum_{i=1}^n P_i(E_\gamma, U), \quad (5)$$

where the term P_i stands for both the probability of the i th γ ray being the most energetic and its energy distribution.

The exact expression for P_i is

$$\begin{aligned} P_i(E_\gamma, U) = & \prod_{j=1; j \neq i}^n \int_0^{\min\{E_\gamma, U - \sum_{k=1}^{j-1} E_k\}} dE_j \\ & \times \frac{\phi(E_j, U - \sum_{k=1}^{j-1} E_k)}{F(U - \sum_{k=1}^{j-1} E_k)} \\ & \times \frac{\phi(E_\gamma, U - \sum_{k=1}^{i-1} E_k)}{F(U - \sum_{k=1}^{i-1} E_k)}. \end{aligned} \quad (6)$$

The product of probabilities of other γ rays having smaller energy is considered through the multiple integrations and the first term in the second line. The last term is the energy distribution of the i th γ ray. Note that for every transition the intrinsic excitation energy corresponds to the initial U minus the energy summation of the previously emitted γ rays. Once Eq. (6) is expanded, E_i must be replaced by E_γ . Refer to [30] for further details on the derivation.

An energy-ordered spectrum from a Monte Carlo simulation of the nuclear decay of ^{170}Hf using the Fermi gas level density and the giant dipole resonance γ strength with the parameters in Ref. [18] is presented in Fig. 1 (solid line). The spectrum shape has been computed with Eq. (5) for $n = 2, 3$, and 4 and results have been depicted with dashed lines. The simulation is satisfactorily reproduced by the previous calculations at energies above an energy threshold. Such a threshold moves to lower energies when taking higher values of n . Consequently, EOS can be properly reproduced in any energy range by choosing n .

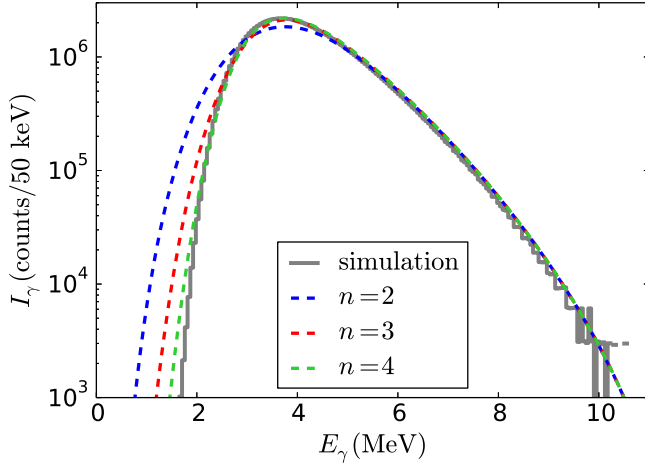


FIG. 1. Energy-ordered spectrum obtained from a Monte Carlo simulation (solid line) of the ^{170}Hf decay for an initial $U = 11$ MeV and the parameters in Ref. [18]. Computed spectrum shape (dashed lines) with Eq. (5) for different n values. The agreement at low energies improves as n increases.

III. SPECTRUM SHAPE FOR THE SPIN-DEPENDENT CASE

The probability density of γ emission is more complex than Eq. (3); it also depends on the spin I of initial and final states, the type of transition regarding the electromagnetic character and multiplicity ($E1$, $M1$, $E2$), and on whether the transition is either statistical or collective. Exactly computing the spectrum shape is a very difficult task due to the multiplicity of phenomena to be included in a detailed probability calculation, however suitable approximations allow to achieve good agreement between analytically calculated spectra and simulated ones.

It was demonstrated with GAMBLE simulations, when taking a slice on excitation energy of $9 < U < 11$ MeV, that the largest contribution to EOS are statistical $E1$ transitions [18]. Therefore, in the following only such transitions are considered. $E1$ transitions can change the nuclear spin by $\Delta I = -1, 0, 1$ with $\Delta I = -1$ the most likely. Thus, it is assumed that the first transition is $E1$ $\Delta I = -1$ and that subsequent transitions are statistical $E1$ with an average $\Delta I = 0$ such as in the spin-independent case. Under these approximations, the spectrum shape can be calculated with the spin-independent function using a suitable initial intrinsic excitation energy.

An initial state (I, E) has an intrinsic excitation energy $U = E - E_{\text{yrast}}(I)$, where $E_{\text{yrast}}(I)$ is the energy of the yrast states. The spin-dependent function p_{EOS}^S can be computed with Eq. (5) using an *effective* intrinsic excitation energy of $E - E_{\text{yrast}}(I - 1)$,

$$p_{\text{EOS}}^S(E_\gamma; (I, E)) = p_{\text{EOS}}(E_\gamma, E - E_{\text{yrast}}(I - 1)). \quad (7)$$

In order to test the previous function, a GAMBLE simulation of the decay of the transitional nucleus ^{154}Dy has been performed using the Fermi gas level density with $a = 18.4$ MeV $^{-1}$ [25] and the giant dipole resonance γ strength [21]. The simulation has been carried out for an initial state $(I, E) = (47\hbar, 29.0$ MeV), corresponding to $U = 11.0$ MeV.

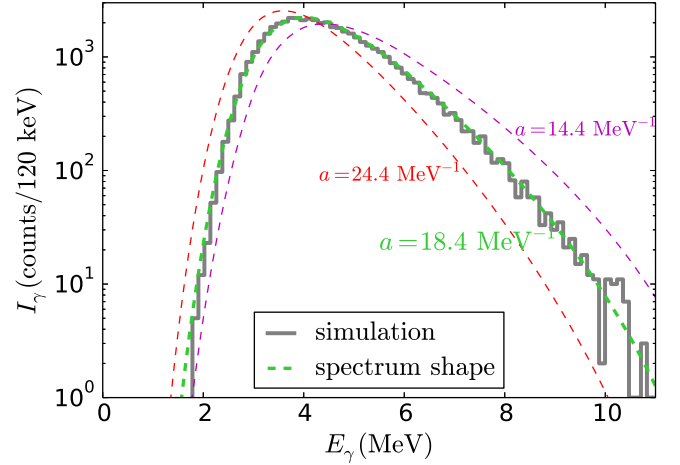


FIG. 2. EOS from GAMBLE simulations of the ^{154}Dy decay (solid line) and calculated spectrum shape with Eq. (7) (dashed lines) for an initial state $(I, E) = (47\hbar, 29.0$ MeV); $U = 11$ MeV. A good agreement between simulated data and the calculated shape with the proper a is observed (green line). On the contrary, no agreement is obtained for other a values (red and purple lines).

The number of simulated cascades is 5×10^4 . The EOS constructed from simulated data is shown in Fig. 2 with a solid line. The function has been numerically computed using Eq. (7) with $n = 4$, and has been plotted with a green dashed line. A good agreement between the simulated spectrum and the calculated shape is observed in the entire energy range, validating the spin-dependent calculated function.

The spectrum shape has also been computed and plotted for $a = 14.4$ and 24.4 MeV $^{-1}$, values different from the GAMBLE input. In this case, correctly, no agreement with the simulated data is obtained. This shows that the computed spectrum shape is sensitive to the physical parameters, in this case to a , and can be used to infer them from comparisons with experimental data. The quality of the fit and the extraction of physical parameters will be further discussed in Sec. V.

IV. BROAD INITIAL DISTRIBUTION OF STATES

The excited states produced after fusion-evaporation reactions have a wide distribution of energy and spin [19]. This case does not correspond to a state with well defined (I, E) as discussed in the previous section, thus the calculated function cannot be directly applied. The situation can be improved by using the Hk technique [20], which allows to select cascades coming from a reduced region in the (I, E) plane. In Fig. 3(a), a realistic distribution of states obtained with the Hk technique [19] is presented with contours on the (I, E) plane. The red lines depict yrast states.

In order to analyze experimental spectra obtained under more general conditions, the spectrum shape has to be computed for an initial distribution of states $\rho_0(I, E)$. This distribution may include the Hk region explained above, but also more general experimental conditions as differential effects in the population of the entry states after fusion-evaporation reactions [32]. This is done by integrating p_{EOS}^S weighted

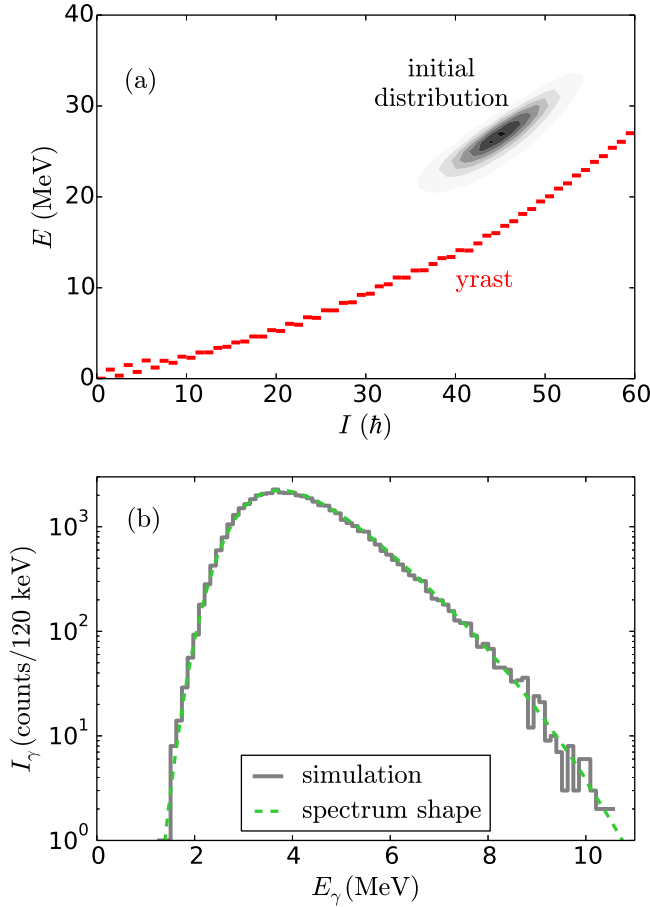


FIG. 3. (a) Distribution of initial states $\rho_0(I, E)$ given by the Hk technique [19]. (b) Simulated EOS for the ^{154}Dy decay and calculated spectrum shape with Eq. (9) and taking $n = 4$. An agreement between simulated data and calculation is observed.

with ρ_0 ,

$$p_{\text{EOS}}^S(E_\gamma; \rho_0(I, E)) = \sum_{I=0}^{\infty} \int_{E_{\text{yrast}}}^{\infty} dE p_{\text{EOS}}^S(E_\gamma; (I, E)) \rho_0(I, E). \quad (8)$$

In the previous section, the calculated function for a state (I, E) has been approximated with an effective internal energy $U' = E - E_{\text{yrast}}(I - 1)$. Correspondingly, it is convenient to simplify Eq. (8) for obtaining only an integration on U' of the form

$$p_{\text{EOS}}^S(E_\gamma; \rho_0(I, E)) = \int dU' \rho_0(U') p_{\text{EOS}}(E_\gamma, U'), \quad (9)$$

where $\rho_0(U')$ is an effective distribution, and p_{EOS} is the spin-independent calculated function from Eq. (5). For a population not overlapping with the yrast states, the effective distributions can be obtained with

$$\rho_0(U') = \sum_{I=0} \rho_0(I, U' + E_{\text{yrast}}(I - 1)). \quad (10)$$

A GAMBLE simulation of the ^{154}Dy decay has been performed for the realistic distribution of states shown in Fig. 3(a) and 5×10^4 cascades. The simulated EOS is shown in

Fig. 3(b) with a solid line. The calculated spectrum shape has been obtained with Eqs. (9) and (10) taking $n = 4$ for the p_{EOS} computation. The result plotted with a dashed line matches the simulation.

The agreement obtained in both cases, Figs. 2 and 3(b), shows that the calculation of the EOS shape works suitably for realistic cases, even when experimental conditions are taken into account.

V. EXTRACTION OF LEVEL DENSITY PARAMETER

The experimental investigation of the nuclear continuum using EOS requires the assessment of the fit quality in order to extract physical parameters and to prove nuclear models. In this section, the level density parameter a is extracted from comparisons of the computed spectrum shape with simulated data for various cases. This shows that the computed function properly recovers the EOS and that physical parameters describing the nucleus can be extracted with a good accuracy.

The reduced χ -squared χ_r^2 between the fitting function and simulated spectrum has been computed with

$$\chi_r^2 = \frac{1}{m} \sum_{j=i_{\min}}^{i_{\max}} \frac{(y_j^{\text{theo}} - y_j^{\text{exp}})^2}{y_j^{\text{theo}}}, \quad (11)$$

where the experimental values y_j^{exp} correspond to the simulated histogram (GAMBLE), the theoretical values y_j^{theo} correspond to the computed spectrum shape multiplied times the number of simulated cascades and energy bin of the histogram. $m = i_{\max} - i_{\min}$ is the number of bins under consideration. The energy range for the calculation, $E_\gamma > 2$ MeV, is chosen such that the fitting function for $n = 4$ converges.

The spectrum shape is computed for multiple values of the level density parameter a . The best value and its error bar are obtained from the values of χ_r^2 [33]. The procedure is presented for the initial state $(I, E) = (47\hbar, 29.0$ MeV) discussed in Sec. III. χ_r^2 is computed for fitting functions with a in the range 18.0–19.0 MeV $^{-1}$. The results are shown in Fig. 4. The minimum at 18.8 MeV $^{-1}$ provides the optimal a obtained from the comparison process, whereas the value $\chi_r^2 = 1.63$ indicates a good agreement. The error bar ± 0.6 MeV $^{-1}$, indicated as a shadowed area in the figure, is estimated from the a values at which χ_r^2 increases by 1 above the minimum. Note that the input value of the simulation $a = 18.4$ MeV $^{-1}$ depicted in blue is within the error bars.

The same process has been repeated for various initial states and a different number of cascades N . The results are summarized in Table I. Higher statistics reduces the error bar as expected. For other (I, E) initial states as well as for the Hk initial distribution discussed in Sec. IV, the fit is also good and the extracted a is in agreement with the input value to the simulation.

VI. APPLICATION TO ANALYSIS OF PHASE TRANSITIONS

Theoretical models predict phase transitions at high excitation energy and spin. For example, in Ref. [17] a transition between oblate and prolate states in ^{154}Dy has been predicted.

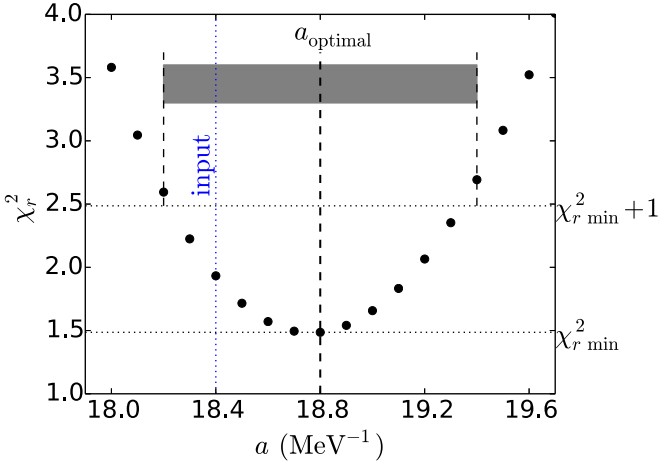


FIG. 4. χ_r^2 according to Eq. (11) as a function of the level density parameter a . Optimal a is at the minimum χ_r^2 and the error bar is estimated as the variation of a that increases χ_r^2 by one.

For low excitation energy and spin, oblate states are predicted, whereas for high E or I prolate states are expected. Despite the strong interest in these phenomena, their experimental investigation is still challenging; the method to locate the transition boundary in the spin and excitation energy plane, as well as to determine the physical parameters describing both regions is still unclear. In this section, the possibility to use EOS jointly with the computed spectrum shape to analyze phase transitions and to extract information from experimental data is discussed.

In the present work two regions of the ^{154}Dy continuum characterized by different level density parameters a are considered. In one of the regions $a = 18.4 \text{ MeV}^{-1}$ [21] and as a test value $a = 22.1 \text{ MeV}^{-1}$ is taken in the nearby region. The second value has no experimental support but it provides 20% difference useful for assessing the following procedure. A phase transition is included at an intrinsic excitation energy $U = 3.5 \text{ MeV}$, as shown by the $a(U)$ dependence in Fig. 5(a). This recreates the experimental condition of feeding high E states in the prolate region, whose decay goes through the oblate one.

The original GAMBLE code has been modified to include this type of variation of the level density parameter. The con-

TABLE I. Extracted a values and minimum χ_r^2 from the fit to simulated EOS. Different initial states and number of cascades N are presented. The extracted values are in agreement with the input value of simulations $a = 18.4 \text{ MeV}^{-1}$. $\chi_r^2 \approx 1$ indicates a good fit quality.

	$E(\text{MeV})$	$I(\hbar)$	N	$a(\text{MeV}^{-1})$	χ_r^2
	29	47	5×10^4	18.8 ± 0.6	1.49
	29	47	2.5×10^5	18.7 ± 0.3	1.27
	29	47	5×10^5	18.6 ± 0.2	1.34
	24	47	5×10^4	18.7 ± 0.5	1.32
	27	47	5×10^4	18.6 ± 0.6	1.21
$Hk \rightarrow$	25.0 ± 2	44 ± 4	5×10^4	18.7 ± 0.6	1.23

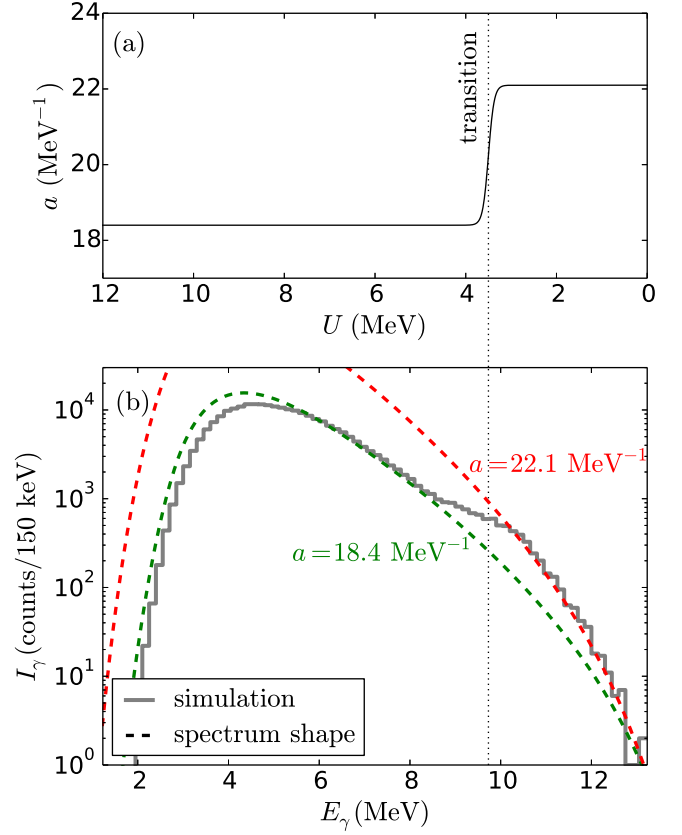


FIG. 5. (a) Input $a(U)$ for ^{154}Dy . A phase transition takes place at $U = 3.5 \text{ MeV}$. (b) The simulated EOS (solid) shows a bump around 9.7 MeV indicating the phase transition. The renormalized calculated functions (dashed) with $a = 18.4$ and 22.1 MeV^{-1} satisfactorily reproduce the spectrum shape below and above the transition bump, respectively.

tinuum decay has been simulated for an initial state $(I, E) = (47\hbar, 30.5 \text{ MeV})$ corresponding to $U = 12.5 \text{ MeV}$. The number of cascades is 2.5×10^5 . The simulated EOS in Fig. 5(b) shows a bump; a new feature not observed in spectra with constant a , cf. Figs. 1, 2, and 3(b). The bump at around $E_\gamma \approx 9.7 \text{ MeV}$ is an indication of the phase transition; indeed, that energy approximates the effective excitation energy $E - E_{\text{yrast}}(I - 1) = 13.2 \text{ MeV}$ minus the energy at the transition 3.5 MeV . The two plots in Fig. 5 have been aligned to make this point explicit. From this analysis, it can be concluded that phase transitions along U can be identified and located with EOS.

In order to extract a , the function of Eq. (7) with $a = 18.4$ and 22.1 MeV^{-1} has been computed. After including a suitable normalization, they have been plotted in Fig. 5(b) with green and red dashed lines, respectively. The function reproduces the EOS above and below 9.7 MeV with the proper a , implying that it is possible to extract the parameters describing both regions.

VII. CONCLUSIONS

In this work an experimental method for investigating nuclei at high energy and spin has been reviewed. The

computation of the shape of energy-ordered spectra has been presented and extended to cover experimentally relevant cases. This provides the mathematical tool required for analyzing data of the nuclear continuum.

The spin-independent spectrum shape [30] has been successfully used to reproduce GAMBLE spectra in the entire energy range. Moreover, a spectrum obtained from an initial state distribution provided by the Hk technique has also been reproduced, showing that the function may be used to analyze spectra including realistic experimental conditions. The level density parameter a has been extracted from simulated spectra. The obtained values agree well with simulation inputs and have a better precision than previous approaches to the spectrum shape. As an additional plus, the χ_r^2 analysis has asserted the reliability of the procedure.

It has been shown that nuclear phase transitions along the excitation energy could be identified using the Hk -EOS

technique and that there is a chance to determine the energy value at which the transition happens together with the corresponding values of the level density parameters of the two regions.

In this work analytical procedures on the approximation to the EOS shape have been presented. The application of this method requires large granularity arrays covering a solid angle as close as possible to 4π with high efficiency at γ energies up to 15 MeV as it was shown for the GASP array [19]. Nowadays, one promising case array is the one envisaged in the original proposal for PARIS [34], presently under test and development. The capabilities of the array for the reconstruction of the Hk regions have to be tested by numerical simulations in order to evaluate the potential for future experimental proposals. The combination of the results presented in this paper with an experimental evaluation of the Hk technique would provide a complete experimental method for studies of the continuum region.

-
- [1] Y. Alhassid, J. Zingman, and S. Levit, *Nucl. Phys. A* **469**, 205 (1987).
- [2] S. Levit and Y. Alhassid, *Nucl. Phys. A* **413**, 439 (1984).
- [3] V. Martin and J. L. Egido, *Phys. Rev. C* **51**, 3084 (1995).
- [4] A. L. Goodman, *Phys. Rev. C* **33**, 2212 (1986).
- [5] A. L. Goodman, *Nucl. Phys. A* **352**, 30 (1981).
- [6] S. Goriely, P. Dimitriou, M. Wiedeking, T. Belgia, R. Firestone, J. Kopecky, M. Krticka, V. Plujko, R. Schwengner, S. Siem, H. Utsunomiya, S. Hilaire, S. Péru, Y. S. Cho, D. M. Filipescu, N. Iwamoto, T. Kawano, V. Varlamov, and R. Xu, *Eur. Phys. J. A* **55**, 172 (2019).
- [7] L. Henden, L. Bergholt, M. Guttormsen, J. Rekstad, and T. Tveter, *Nucl. Phys. A* **589**, 249 (1995).
- [8] A. Schiller, L. Bergholt, M. Guttormsen, E. Melby, S. Messelt, J. Rekstad, and S. Siem, *Phys. Scr.* **2000**, 144 (2000).
- [9] M. Guttormsen, E. Melby, J. Rekstad, S. Siem, A. Schiller, T. Lönnroth, and A. Voinov, *J. Phys. G: Nucl. Part. Phys.* **29**, 263 (2003).
- [10] M. Guttormsen, A. Bagheri, R. Chankova, J. Rekstad, S. Siem, A. Schiller, and A. Voinov, *Phys. Rev. C* **68**, 064306 (2003).
- [11] U. Agvaanluvsan, A. Schiller, J. A. Becker, L. A. Bernstein, P. E. Garrett, M. Guttormsen, G. E. Mitchell, J. Rekstad, S. Siem, A. Voinov, and W. Younes, *Phys. Rev. C* **70**, 054611 (2004).
- [12] H. K. Toft, A. C. Larsen, U. Agvaanluvsan, A. Bürger, M. Guttormsen, G. E. Mitchell, H. T. Nyhus, A. Schiller, S. Siem, N. U. H. Syed, and A. Voinov, *Phys. Rev. C* **81**, 064311 (2010).
- [13] M. Guttormsen, B. Jurado, J. N. Wilson, M. Aiche, L. A. Bernstein, Q. Ducasse, F. Giacoppo, A. Görgen, F. Gunsing, T. W. Hagen, A. C. Larsen, M. Lebois, B. Leniau, T. Renstrøm, S. J. Rose, S. Siem, T. Tornyi, G. M. Tveten, and M. Wiedeking, *Phys. Rev. C* **88**, 024307 (2013).
- [14] T. G. Tornyi, M. Guttormsen, T. K. Eriksen, A. Görgen, F. Giacoppo, T. W. Hagen, A. Krasznahorkay, A. C. Larsen, T. Renstrøm, S. J. Rose, S. Siem, and G. M. Tveten, *Phys. Rev. C* **89**, 044323 (2014).
- [15] T. Renstrøm, H.-T. Nyhus, H. Utsunomiya, R. Schwengner, S. Goriely, A. C. Larsen, D. M. Filipescu, I. Gheorghe, L. A. Bernstein, D. L. Bleuel, T. Glodariu, A. Görgen, M. Guttormsen, T. W. Hagen, B. V. Kheswa, Y.-W. Lui, D. Negi, I. E. Ruud, T. Shima, S. Siem, K. Takahisa, O. Tesileanu, T. G. Tornyi, G. M. Tveten, and M. Wiedeking, *Phys. Rev. C* **93**, 064302 (2016).
- [16] N. Q. Hung, N. D. Dang, and L. T. Quynh Huong, *Phys. Rev. Lett.* **118**, 022502 (2017).
- [17] W. C. Ma, V. Martin, T. L. Khoo, T. Lauritsen, J. L. Egido, I. Ahmad, P. Bhattacharyya, M. P. Carpenter, P. J. Daly, Z. W. Grabowski, J. H. Hamilton, R. V. F. Janssens, D. Nisius, A. V. Ramayya, P. G. Varmette, and C. T. Zhang, *Phys. Rev. Lett.* **84**, 5967 (2000).
- [18] F. Cristancho, *Heavy Ion Phys.* **2**, 299 (1995).
- [19] E. Merchán and F. Cristancho, *Phys. Scr. T* **125**, 184 (2006).
- [20] C. Baktash, M. Halbert, D. Hensley, N. Johnson, I. Lee, J. McConnell, and F. McGowan, *Nucl. Phys. A* **520**, c555 (1990).
- [21] G. A. Leander, *Phys. Rev. C* **38**, 728 (1988).
- [22] D. M. Brink, Ph.D. thesis, University of Oxford, 1955.
- [23] P. Axel, *Phys. Rev.* **126**, 671 (1962).
- [24] G. A. Bartholomew, E. D. Earle, A. J. Ferguson, J. W. Knowles, and A. M. Lone, in *Advances in Nuclear Physics*, Vol. 7, edited by M. Baranger and E. Vogt (Pergamon Press, New York, 1973), Chap. 4, p. 229.
- [25] D. W. Lang, *Nucl. Phys.* **77**, 545 (1966).
- [26] F. Cristancho and J. P. Urrego, *Acta Phys. Hung. A: Heavy Ion Phys.* **16**, 75 (2002).
- [27] R. F. G. Ruiz and F. Cristancho, *AIP Conf. Proc.* **1265**, 106 (2010).
- [28] B. Arnold, N. Balakrishnan, and H. Nagaraja, *A First Course in Order Statistics*, Classics in Applied Mathematics (Society for Industrial and Applied Mathematics, Philadelphia, Pennsylvania, United States, 2008).
- [29] E. Gumbel, *Statistics of Extremes*, Dover Books on Mathematics (Dover Publications, Mineola, New York, 2004).
- [30] J. R. Pinzón and F. Cristancho, in *IX Latin American Symposium on Nuclear Physics and Applications*, edited by R. Alarcon, E. Ayala, C. Granja, and N. Medina, AIP Conf. Proc. No. 1423 (AIP, New York, 2012), p. 53.

- [31] G. A. Leander, *Comput. Phys. Commun.* **47**, 311 (1987).
- [32] F. Cristancho and K. Lieb, *Nucl. Phys. A* **524**, 518 (1991).
- [33] D. Rogers, *Nucl. Instrum. Methods* **127**, 253 (1975).
- [34] A. Maj, F. Azaiez, D. Jenkins, C. Schmitt, O. Stezowski, J. Wieleczko, D. Balabanski, P. Bednarczyk, S. Brambilla, F. Camera, D. Chakrabarty, M. Chelstowska, M. Ciemala, S. Courtin, M. Csatlos, Z. Dombradi, O. Dorvaux, J. Dudek, M. Erduran, S. Ertuerk, B. Fornal, S. Franchoo, G. Georgiev, J. Gulyas, S. Harissopoulos, P. Joshi, M. Kicinska-Habior, M. Kmiecik, A. Krasznahorkay, G. Kumar, S. Kumar, M. Labiche, I. Mazumdar, K. Mazurek, W. Meczynski, S. Myalski, V. Nanal, P. Napiorkowski, J. Peyre, J. Pouthas, O. Roberts, M. Rousseau, J. Scarpaci, A. Smith, I. Stefan, J. Strachan, D. Watts, M. Zieblinski, and Paris Collaboration, *Acta Phys. Pol. B* **40**, 565 (2009).